

Purdue University Purdue e-Pubs

Birck and NCN Publications

Birck Nanotechnology Center

June 2008

'Living cantilever arrays' for characterization of mass of single live cells in fluids

Kidong Park

Purdue University, park35@purdue.edu

Jaesung Jang

Department of Mechanical Engineering, Chung-Ang University

Daniel Irimia

Massachusetts Gen Hosp, Shriners Hosp Children, Ctr Engn Med & Surg Serv, BioMEMS Resource Ctr

Jennifer Sturgis

Purdue University, jesturgis@purdue.edu

James Lee

Ohio State Univ, Dept Chem Engn

See next page for additional authors

Follow this and additional works at: <http://docs.lib.purdue.edu/nanopub>

Park, Kidong; Jang, Jaesung; Irimia, Daniel; Sturgis, Jennifer; Lee, James; Robinson, J. Paul; Toner, Mehmet; and Bashir, Rashid, "Living cantilever arrays' for characterization of mass of single live cells in fluids" (2008). *Birck and NCN Publications*. Paper 147. <http://docs.lib.purdue.edu/nanopub/147>

This document has been made available through Purdue e-Pubs, a service of the Purdue University Libraries. Please contact epubs@purdue.edu for additional information.

Authors

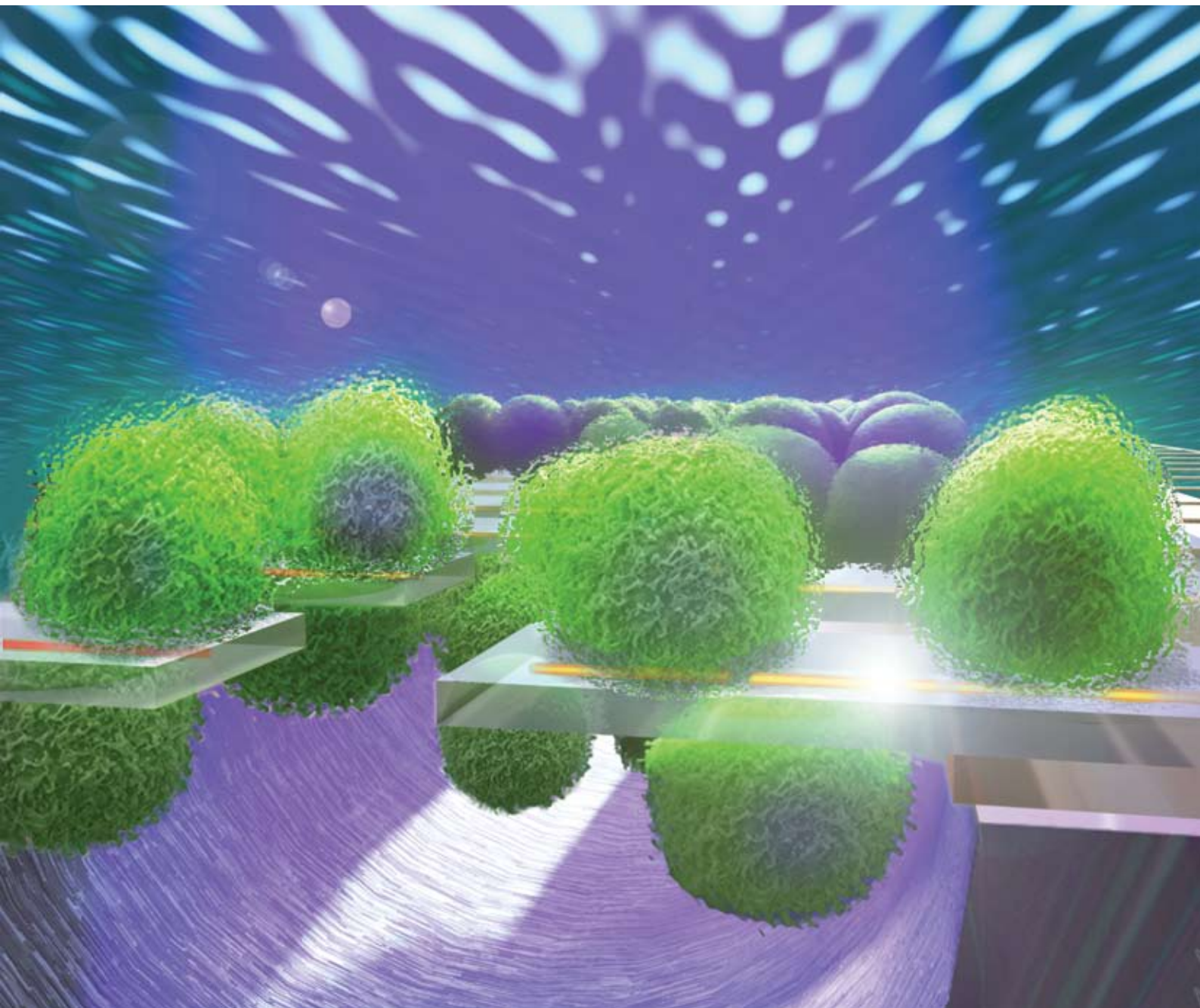
Kidong Park, Jaesung Jang, Daniel Irimia, Jennifer Sturgis, James Lee, J. Paul Robinson, Mehmet Toner, and Rashid Bashir

Lab on a Chip

Miniaturisation for chemistry, biology & bioengineering

www.rsc.org/loc

Volume 8 | Number 7 | July 2008 | Pages 993–1228



ISSN 1473-0197

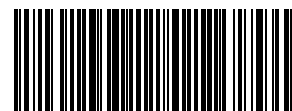
RSC Publishing

Suh
Tutorial Review: Cell research with
modified channels

Bashir
Living cantilever arrays

Willis
Monolithic valves and pumps for
planetary exploration

Desai
Controlled release of oral therapeutics



1473-0197(2008)8:7;1-X

'Living cantilever arrays' for characterization of mass of single live cells in fluids†

Kidong Park,^{a,b} Jaesung Jang,^c Daniel Irimia,^d Jennifer Sturgis,^{e,f} James Lee,^g J. Paul Robinson,^{e,f,h} Mehmet Toner^d and Rashid Bashir^{*i}

Received 3rd March 2008, Accepted 12th May 2008

First published as an Advance Article on the web 11th June 2008

DOI: 10.1039/b803601b

The size of a cell is a fundamental physiological property and is closely regulated by various environmental and genetic factors. Optical or confocal microscopy can be used to measure the dimensions of adherent cells, and Coulter counter or flow cytometry (forward scattering light intensity) can be used to estimate the volume of single cells in a flow. Although these methods could be used to obtain the mass of single live cells, no method suitable for directly measuring the mass of single adherent cells without detaching them from the surface is currently available. We report the design, fabrication, and testing of 'living cantilever arrays', an approach to measure the mass of single adherent live cells in fluid using silicon cantilever mass sensor. HeLa cells were injected into microfluidic channels with a linear array of functionalized silicon cantilevers and the cells were subsequently captured on the cantilevers with positive dielectrophoresis. The captured cells were then cultured on the cantilevers in a microfluidic environment and the resonant frequencies of the cantilevers were measured. The mass of a single HeLa cell was extracted from the resonance frequency shift of the cantilever and was found to be close to the mass value calculated from the cell density from the literature and the cell volume obtained from confocal microscopy. This approach can provide a new method for mass measurement of a single adherent cell in its physiological condition in a non-invasive manner, as well as optical observations of the same cell. We believe this technology would be very valuable for single cell time-course studies of adherent live cells.

Introduction

Recent advances in micro-system technology offer the possibility of handling, manipulating and characterizing single cells for various applications. Many efforts are focused on the measurement of the physical properties of single cells, which can open new areas of research in biological and medical science.

Physiologically important properties of a cell include its size and mass, which are closely intertwined with various physiological processes of cells. Especially, the cell mass is directly related to the synthesis and accumulation of proteins, replication of DNA, and other large molecules inside the cell during growth and differentiation. Several methods, such as optical microscopy, confocal microscopy and the suspended microchannel resonator,^{1,2} are available to estimate or directly measure the mass of single cells in suspension. By contrast, no method is available for measuring an adherent cell mass directly, while keeping the cell attached on a surface.

In principle, a cell mass can be indirectly estimated by multiplying the cell volume and the cell mass density, assuming a constant density. However, it is shown that the mass density of a cell is not constant through its cell cycle³⁻⁵ and thus indirect estimation of cell mass can be inaccurate. Many researchers working on a cell's size regulation or growth rate, simply use cell volume⁶⁻⁹ as a primary indicator of the cell size. Coulter counter or flow cytometry (FSC—forward scattered light intensity parameter) are widely used to measure the relative volume of cells in a flow. A Coulter counter measures the relative volume of a single cell by detecting the change in electrical conductance of a small aperture as cell suspension is flowing through.¹⁰ Due to the insulating properties of the cell, the cell traversing the pore decreases the effective cross-section of the conductive channel and a corresponding change in the electrical resistance of the pore. The FSC parameter in flow cytometry measures the light scattered in the forward

^aBirk Nanotechnology Center, Purdue University, West Lafayette, IN, 47907, USA

^bSchool of Electrical and Computer Engineering, Purdue University, West Lafayette, IN, 47907, USA

^cNow at Department of Mechanical Engineering, Chung-Ang University, Seoul, 156-756, S. Korea

^dBioMEMS Resource Center, Center for Engineering in Medicine and Surgical Services, Massachusetts General Hospital, Shriners Hospital for Children, and Harvard Medical School, Boston, MA, 02129, USA

^eBindley Biosciences Center, Purdue University, West Lafayette, IN, 47907, USA

^fDepartment of Basic Medical Sciences, Purdue University, West Lafayette, IN, 47907, USA

^gDepartment of Chemical Engineering, The Ohio State University, Columbus, OH, 43210, USA

^hWeldon School of Biomedical Engineering, Purdue University, West Lafayette, IN, 47907, USA

ⁱMicro and Nanotechnology Laboratory, Department of Electrical and Computer Engineering & Bioengineering, University of Illinois at Urbana-Champaign, Urbana, IL, 61801, USA. E-mail: rbashir@uiuc.edu; Fax: +1-217-244-6375; Tel: +1-217-333-3097

† Electronic supplementary information (ESI) available: Fig. S1 and S2, and movies 1 and 2. See DOI: 10.1039/b803601b

direction as a cell passes through a laser beam. Since the FSC parameter of a spherical cell is proportional to the volume,¹¹ it is primarily used to measure the cell volume especially for obtaining the correlation between the cell volume and other cell parameters, such as the SSC (side scattering light intensity) parameter or the intensities of certain fluorescence signals.^{12,13} The suspended microchannel resonator^{1,2} can directly obtain a cell mass, by measuring the resonance frequency of a suspended microchannel structure while the suspended cell passes through the channel.

Although the above methods are suitable for obtaining the size or mass distribution of a large population of cells, these methods are not suitable for time varying studies on the same single cell. Furthermore, it is not possible to get optical images of the same cell as a function of time, which can easily identify the status of the cell. These flow-based methods also require the cells to be in suspension as they flow through the detection area. For adherent cells, such as fibroblast and epithelial cells, this means that cells should be detached from the surface prior to the measurement, which can cause significant physiological changes to the cell.

One of the direct methods for measuring cell mass is the use of micromechanical resonant cantilever mass sensors for measurement and characterization of single cells. The resonance frequency of a cantilever is inversely proportional to the square root of the mass. Therefore, the mass of the entities attached to the cantilever can be directly calculated from the resonance frequency of the cantilever. In earlier works, a microcantilever was used to measure the relative humidity and the mercury vapor^{14,15} by the resonance frequency shift. Since then, many researchers have used the cantilever as a highly sensitive sensor element in various applications.¹⁶ The detection or the mass measurement of many biologically important entities such as DNA, viruses, bacteria, spores and micro-beads have been successfully demonstrated.^{17–23} Moreover, the living mammalian cell and the microcantilever were integrated for detecting cytotoxic molecules²⁴ or investigating the contractile force of cultured myotubes.²⁵ Recently, a suspended microchannel resonator^{1,2} was demonstrated with sub-femtogram resolution and the mass of a single bacterial cell and a human red blood cell in suspension were successfully measured. However, to the best of our knowledge, the use of a cantilever mass sensor for measurement of a single adherent cell while culturing the cell on the cantilever has not been demonstrated. For adherent cells cultured on the cantilever surface, this method can be used to measure the cell mass in its physiological conditions, even without detaching the cell from the surface. Therefore, the mass of the cell can be measured with little or no side effect on cell physiology and potentially can be repetitively measured over time to track the growth rate of single cells.

In this study, we demonstrate a new platform for the mass measurement and optical observation of single cells in their physiological conditions using a cantilever mass sensor. This 'Living Cantilever Array' platform incorporates silicon cantilevers and is encapsulated in a PDMS microfluidic channel, as shown in Fig. 1. HeLa cells were captured on the functionalized cantilevers with positive dielectrophoresis, and cultured on the cantilevers for up to 7 days before measuring the resonance frequencies of the cantilevers. The mass of a single HeLa

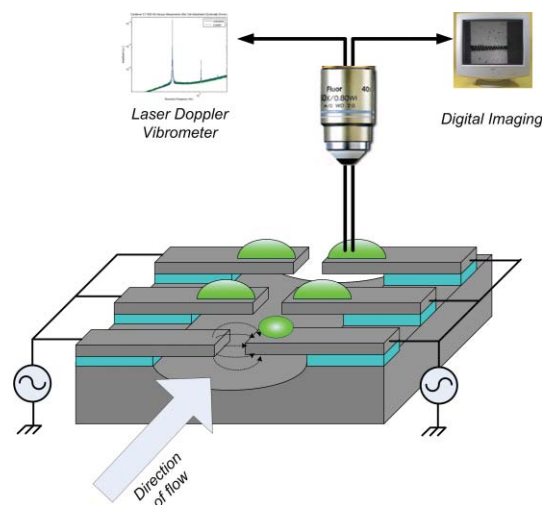


Fig. 1 Schematic diagram of living cantilever array. Target cells in suspension are captured and immobilized on the cantilever. Then the cells are cultured and the mass of a cell on a cantilever is measured *via* the resonance frequency shift of a cantilever.

cell was extracted from the resonance frequency shift of the cantilever and compared with the mass calculated from the cell density from the literature and the cell volume from confocal microscopy.

Materials and methods

Fabrication of the silicon cantilever array

Key steps of the overall fabrication process are presented in Fig. 2(a). The starting material was a 4 inch diameter SOI (silicon-on-insulator) wafer with a 240 nm silicon layer, a 400 nm buried oxide layer, and a 500 μm silicon substrate. The wafer was thoroughly cleaned and the cantilever patterns were defined with a first lithography step on the SOI silicon layer. The silicon layer was then etched with RIE (reactive ion etching) to transfer the photoresist pattern, as shown in step (I) in Fig. 2(a). To make an electrical contact to the substrate, etch windows were defined on the buried oxide by the second lithography step and then the exposed buried oxide layer was etched to produce contact windows on the substrate layer as in shown step (II). To increase the electrical conductivity of the cantilevers and the exposed substrate, the wafer was ion implanted with 10^{14} cm^{-2} of boron at 10 keV and annealed at 900 $^{\circ}\text{C}$ for 30 min. After annealing, a third lithography was performed for a subsequent lift-off process. A Cr/Au layer with total 1 μm thickness was deposited and patterned with the lift-off process to form metal electrodes and wire-bonding pads as in step (III). Next, etch windows for isotropic XeF_2 etch were defined with the fourth lithography step. The wafer was diced into individual dies and the dies were thoroughly rinsed with DI water to remove the debris and impurities from the dicing process. The buried oxide layer was etched to expose the substrate layer as in step (IV) and the exposed substrate layer was etched with XeF_2 to release the cantilevers as shown in step (V). After releasing the cantilevers by XeF_2 etching, the buried oxide layer beneath the cantilever and the photoresist on top of the cantilever were removed as shown in step (VI). Then the device was dried with CPD (critical

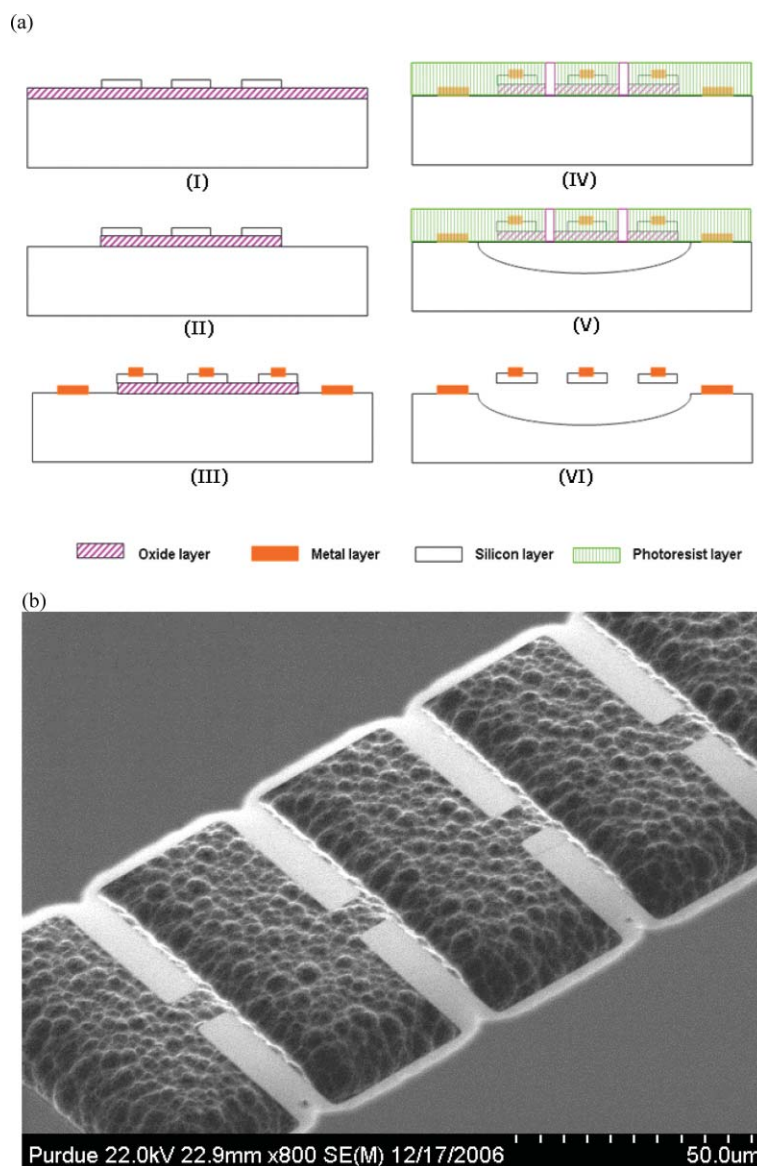


Fig. 2 Fabrication process for the silicon cantilever array. (a) Cross-sectional diagram of the key fabrication process steps. (b) Angled FESEM image of the released cantilevers in a linear array.

point dryer) to avoid stiction between the suspended cantilevers and the substrate. Fig. 2(b) shows an FESEM (field emission scanning electron microscopy) image of the released cantilevers. The die was then attached to a custom made PCB (printed circuit board) with epoxy adhesive and wire-bonded to the PCB for electrical connection. A PDMS cover was fabricated from an SU-8 master which was 50 μm high and 2500 μm wide, and tubings were attached to the PDMS cover. Finally, the PDMS cover with tubings was attached to the silicon surface to complete the device fabrication.

Experimental setup and protocol

The fabricated cantilevers were 25–40 μm long, 10 μm wide and 240 nm thick. As shown in Fig. 1, two sets of cantilevers, opposing to each other, were connected to external sinusoidal power sources with a 180° phase difference to produce a

non-uniform electric field between the opposing cantilevers for dielectrophoresis. Through the transparent PDMS cover, the cantilevers could be observed for microscope imaging and resonance frequency measurement by a LDV (Laser Doppler Vibrometer, MSV-300, Polytech PI). The LDV measures the velocity of the cantilever from the interference between the laser beam reflected from the cantilever surface and the reference laser beam.

HeLa cells were used as a model cell line in the experiment. HeLa cells are immortal human cervical cancer cells, which are one of the most widely used cancer cells.²⁶ HeLa cells were cultured with DMEM (Dulbecco's Modified Eagle's Medium/Nutrient Mixture F-12 Ham, Sigma Aldrich, USA) with 10% FBS (fetal bovine serum, Sigma Aldrich, USA) at 37 °C and 5% CO₂. When the cells became confluent, they were detached by trypsin (0.25% trypsin/1 mM EDTA, Invitrogen/Gibco, USA) and sub-cultured in 1 : 5–1 : 10 ratio.

Table 1 Summary of the experiment protocol

Degassing and functionalization of cantilevers	(1) Measure resonant frequency of the cantilevers in air (2) Completely fill the device with de-aerated DI water (3) Sterilize with 70% ethanol
Cell preparation and DEP capture	(4) Functionalize the cantilever with poly-L-lysine (5) Feed fresh growth media to cells 4 h before the detachment (6) Detach cells from flask by trypsin (7) Rinse and suspend in low conductive capture media
Culture and LDV measurement	(8) Inject cell suspension and DEP capture with 6 Vpp (volts peak to peak), at 1 Mhz (9) Inject growth media into device and culture in CO ₂ incubator (10) LDV measurement of resonance frequency of cantilever with cell on it within growth media (11) Confocal microscopy (12) Detach cells from the cantilevers and LDV measurement within growth media

The overall protocol for the capture and culture of the cells is shown in Table 1. First, the frequency response of each cantilever was measured in air with LDV. From the measured frequency response, the resonance frequency and the spring constant for each cantilever were characterized. Then, completely deaerated DI water was injected to fill the microfluidic channel without any air bubbles. After the microfluidic channel was completely filled with DI water, the microfluidic channel, the cantilevers and the tubings were sterilized by 70% ethanol. After sterilization, poly-L-lysine solution (20 µg ml⁻¹ in PBS) was injected into the device to functionalize the cantilevers. Poly-L-lysine was attached to negatively charged native oxide surface, since -NH₂ groups in poly-L-lysine are positively charged -NH₃⁺ at pH < 10.²⁷ Growth media (DMEM + 10% FBS) was fed to the cells 4 h before the cells were detached by trypsin. The cells were rinsed twice with low conductivity media (8.5% sucrose + 0.3% glucose in DI water) and suspended in the same media. Then the suspended cells were injected into the device, with the dielectrophoresis signals applied to the cantilevers.²⁸ After capturing HeLa cells with positive DEP, the AC voltage signals were turned off and the growth media was injected into the device to replace the low conductivity media from the cell suspension. The device was then moved into a tissue culture incubator at 37 °C and 5% CO₂ to culture the captured cells.

Every 6–8 h, 100 µl of growth media were injected into the device at 20 µl min⁻¹ and the growth and the status of the cells was observed with a microscope. After 3 days, the vibration spectrums of the cantilevers were measured with the LDV and a confocal microscope was used to obtain 3-dimensional images of the cells on the cantilevers. Then the cells were detached by trypsin and the device was cleaned with enzymatic cleaner (Tergazyme, Alconox, Inc., NY, USA). To obtain the reference resonance frequencies of the same cantilevers, the growth media was injected into the device and the vibration spectrums of the cantilevers without cells were measured with LDV.

LDV measurements and analysis

The LDV was used to measure the vibration of the cantilevers. A large number of recordings were performed on a single cantilever using thermal noise as the excitation source. Fourier transform was performed and averaged to produce a vibration spectrum of the cantilever. In the case of a high quality factor and low viscous damping as in air, the resonance frequency of a cantilever could be easily identified from the vibration spectrum. Fig. 3(a) shows a vibration spectrum using thermal noise excitation of one of the

silicon cantilevers in air. However, in the case of measurement in liquid, it was challenging to determine the resonance frequency due to the high viscous damping and the resulting low quality factor. For this reason, vibration spectrums were measured at the non-moving substrate as well as the cantilever, and the vibration spectrum of the cantilever was divided by that of the substrate to produce the frequency response of the cantilever. Then the frequency response was smoothed to remove the fluctuation and the resonance frequency of the cantilever was extracted. In Fig. 3(b) and (c) the vibration spectrums of a cantilever and substrate in growth media are shown. Fig. 3(d) shows the frequency response of the cantilever before and after smoothing the curve.

To characterize the fabricated cantilevers, the spring constant and the resonance frequency were calculated from the vibration spectrums of each cantilever. The typical equation to obtain the spring constant is as follows;

$$k = E \frac{t^3 b}{4L^3} \quad (1)$$

where E is Young's modulus, t is the thickness, b is the width, and L is the length of a cantilever. However, due to the variation in the XeF₂ isotropic etching, the base region of a cantilever was not etched uniformly and therefore the length of each cantilever varied from the design value. For this reason, eqn (1) was not used to estimate the spring constant. Rather, it is more appropriate to calculate the spring constants of the cantilevers from the LDV measurement in air, using eqn (2) as follows;^{29,30}

$$k = 0.1906 \rho_t b^2 L Q_t \Gamma_i(\omega_t) \omega_t^2 \quad (2)$$

where ρ_t is the density of air, Q_t is the quality factor, Γ_i is the imaginary part of the hydrodynamic function^{29,30} and ω_t is the resonance frequency of the vibration spectrum. In this method, we also assumed the length as an ideal value, which might cause errors in calculating spring constant. However, with eqn (2), spring constant is affected by L whereas in eqn (1), spring constant is affected by L^{-3} . By using eqn (2), we can obtain spring constant values which are less dependent on variations in L for each cantilever. The theoretical resonance frequency of the cantilever in vacuum was obtained from eqn (3), and converted into the theoretical resonance frequency in air, by eqn (4).²⁹

$$f_0 = \frac{3.515}{2\pi} \frac{1}{L^2} \sqrt{\frac{EI}{\rho_c A}} \quad (3)$$

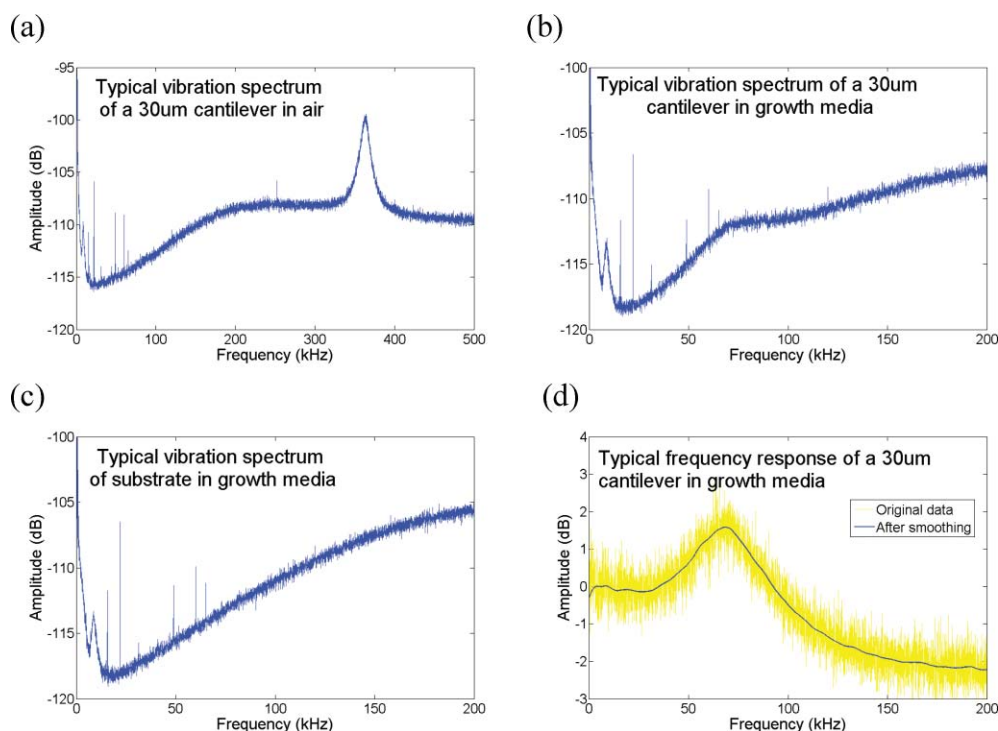


Fig. 3 Typical plots of a vibration spectrum of a cantilever. (a) The vibration spectrum of a 30 μm long cantilever in air. (b), (c) Vibration spectrum of a 30 μm long cantilever and substrate in growth media, respectively. (d) Frequency response of a 30 μm long cantilever in growth media. The yellow line is the frequency response and the blue line is the one after smoothing.

$$\omega_{\text{vac},n} = \omega_{R,n} \left(1 + \frac{\pi \rho_c b}{4 \rho_c I} \Gamma_r(\omega_{R,n}) \right)^{0.5} \quad (4)$$

where I is the moment of the inertia, A is the cross-sectional area of the cantilever, ρ_c is the density of the silicon cantilever, $\omega_{\text{vac},n}$ is resonance angular velocity in vacuum, $\omega_{R,n}$ is resonance angular velocity in the growth media, and Γ_r is the real part of the hydrodynamic function.^{29,30}

For mass measurement, the resonance frequencies of the cantilever with and without a cell were measured in the growth media and the measured frequencies were used to calculate the mass of the cell on the cantilever by eqn (5)¹⁸

$$\Delta m = \frac{k}{4\pi^2} \left(\frac{1}{f_1^2} - \frac{1}{f_0^2} \right) \quad (5)$$

where f_1 is the resonance frequency with the cell and f_0 is the resonance frequency without the cell.

Since the cell mass was distributed over a cantilever and the mass sensitivity of a cantilever varies with the position of the mass,^{31,32} the effective mass calculated by eqn (5) should be compensated by a correctional factor that is derived from the position or the distribution of the mass and the normalized mass sensitivity at each point on the cantilever. The sensitivity is linearly proportional to the square of the vibration amplitude in first resonance mode, as can be seen in the work of Dohn *et al.*³² The normalized sensitivity was obtained by normalizing the square of the vibration amplitude in first resonance mode, so that the normalized sensitivity was 1 at the end of the cantilever.

The normalized vibration amplitude of a cantilever in its n th resonance mode was

$$X_n(x) = \frac{1}{2} \left\{ \begin{aligned} &(\cos k_n x - \cosh k_n x) - \frac{\cos k_n L + \cosh k_n L}{\sin k_n L + \sinh k_n L} \\ &\times (\sin k_n x - \sinh k_n x) \end{aligned} \right\} \quad (6)$$

where x is the position on the cantilever and k_n satisfies $\cos k_n L \cosh k_n L = -1$. The height of the cell from the cantilever surface was measured in the side view of a cell as in Fig. 7(c) and (d) (see later). Then the height was normalized so that the area of the cell outline was 1. This normalized height of the cell, $h_{\text{cell}}(x)$ was used as the cell mass distribution along the cantilever, since the width of the cell was almost constant. Therefore the following correctional factor was used to compensate the effective mass.

$$\alpha = \frac{1}{\int_0^L |X_1(x)|^2 h_{\text{cell}}(x) dx} \quad (7)$$

Results and discussion

Characterization of the cantilever

Prior to capture and mass measurement, each cantilever was characterized by measuring the resonant frequency and the spring constant of the cantilever by LDV in air. Fig. 4 shows the distribution of the resonance frequencies and the spring constants for cantilevers of 3 different lengths. As shown in Fig. 4, the variations in the resonant frequency and the spring constant were larger with the shorter cantilevers. This can be explained by the fact that the variation of the cantilever length was of similar order in all cantilevers and therefore the shorter

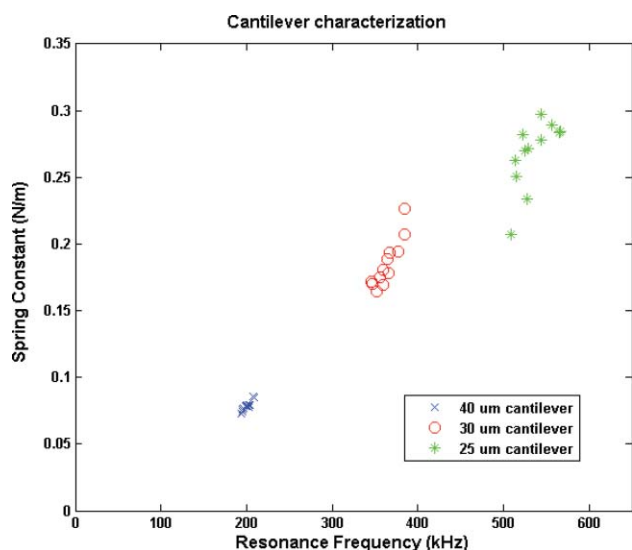


Fig. 4 Distribution of the resonance frequency and the spring constant of the fabricated cantilevers, calculated from LDV measurements.

cantilevers were more affected by length variation. Also, eqn (2) requires the cantilever length to greatly exceed the cantilever width³⁰ but, the ratio between the length and the width was less than 4, which can lead to errors in the spring constants. However, the theoretical and the experimental values were consistent to each other with about 10% differences. The theoretical and the experimental values for the resonance frequency and the spring constant are listed in Table 2.

Capture and culture of HeLa cells on cantilevers

Fig. 5 shows the progression of the capture of HeLa cells by positive dielectrophoresis within the linear microfluidic channel. The cells were suspended in a low conductivity media and two sinusoidal DEP signals of 6 V_{pp} at 1 MHz were applied. The average velocity of the cell suspension was about 0.5–1 mm s⁻¹. After the cells were captured, the DEP signals were turned off and growth media was injected. At this point, the captured cells were attached to the surface only with the adhesion force between the cell and poly-L-lysine molecules coated on the surface. Fibronectin was also considered as an adhesion promoter, but poly-L-lysine was chosen due to its rapid activation of adhesion force with HeLa cell. Poly-L-lysine becomes highly positively charged at physiological conditions and the cells would be captured due to electrostatic interaction.

The captured cells were cultured in a tissue culture incubator. Fig. 6(a) shows the fully grown HeLa cells on the device, after 3 days. The spreading of the cells on the living cantilever array was usually observed after 8 hours, whereas HeLa cells spread in an hour³³ with a standard cell culture protocol. This delayed

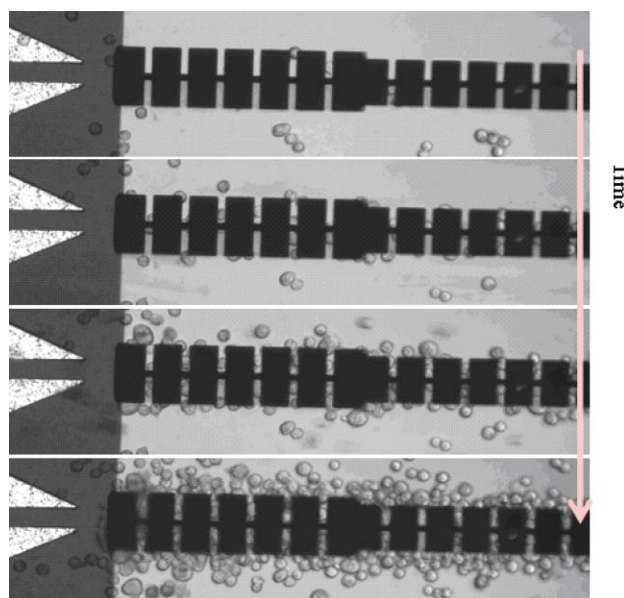


Fig. 5 Capture of HeLa cell with positive dielectrophoresis. The average velocity of the cell suspension was between 0.5–1 mm s⁻¹ and the sinusoidal DEP signals of 6 V_{pp} at 1 MHz were applied. (see ESI Video 1†).

spreading of the captured cells is believed to be from the exposure to lower than optimum temperature and low conductivity media, during the DEP capture process. After the spreading, the growth and the proliferation of the cells were clearly observed. In some cases, due to the cell migration, the cell on the cantilever moved to the surrounding area or the cell on the surrounding area moved onto the cantilever. It usually took 3 days for the cells to grow and to be ready for the following LDV measurement and confocal microscopy. However, in some cases, the captured cells were cultured for up to 7 days to increase the number of cantilevers occupied with cells.

Confocal microscope images

After LDV measurements, for further characterization and as a control measurement, the cells on the cantilever were imaged with a confocal microscope as shown in Fig. 6(b)–(d). The HeLa cells were shown as green, stained with lipophilic fluorescent dye, DiOC63, and the silicon was shown as blue from the reflected optical signal. As can be seen in Fig. 6(b)–(d), many cantilevers were covered with single cells and also many cells were observed inside the trench area and beneath the cantilevers, since the parasitic electric field between substrate and the cantilever generated positive dielectrophoretic force to attract the cells into the trench area. In analyzing the mass of the cell on the cantilever, the 3-dimensional confocal microscope image

Table 2 Comparison of the theoretical and experimental values for the resonance frequency and the spring constant

Length	Resonance frequency (theoretical)/kHz	Resonance frequency (experimental)/kHz	Spring constant (theoretical)/N m ⁻¹	Spring constant (experimental)/N m ⁻¹
40 μm	181.59	202.54 ± 5.84	0.0713	0.0810 ± 0.0043
30 μm	324.11	365.42 ± 13.38	0.1690	0.1840 ± 0.0177
25 μm	467.65	513.90 ± 111.05	0.2920	0.2590 ± 0.0607

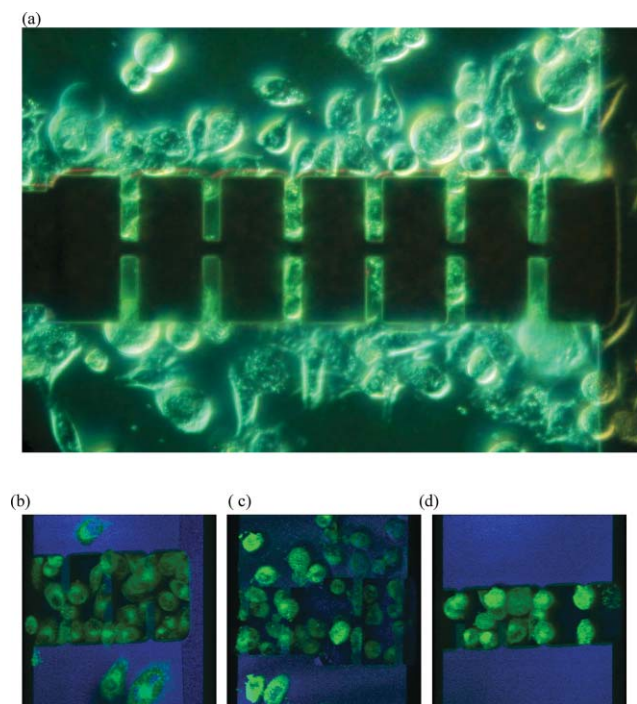


Fig. 6 Cultured cells on the cantilever. (a) Grown HeLa cells in the microfluidic device, after 3 days. (b), (c), (d) Confocal microscopy of living cantilever array. The nucleus can be identified as the hollow space inside each cell. (b) The HeLa cells on 40 μm long cantilevers. (c) HeLa cells on 40 and 30 μm long cantilevers. (d) HeLa cells on 25 μm cantilevers (see ESI Video 2 for 3-D confocal images of (b), (c) and, (d)†).

was used to exclude cantilevers on which cells were attached improperly. Also, the confocal microscope images were used as

a control, to calculate the volume of a cell attached to a specific cantilever to estimate the cell mass.

Mass measurement

Fig. 7(a) and (b) show the measured frequency responses of the cantilevers with and without a cell in the growth media. For each case, the resonant frequency decreased by 2.93 kHz and 5.43 kHz respectively. These frequency shifts correspond to the cell mass of 1.01 ng and 3.57 ng using the procedure described in the previous section.

The measured mass from the frequency response was compared with the estimated value calculated from the cell density and the cell volume. The volume of the cell was measured from the confocal microscope images by Image J (Wayne Rasband, National Institute of Health, USA), and the published value for the density of the cell was used.³ The measured volume of the cell for Fig. 7(a) and (b) were 2349 μm^3 and 3857 μm^3 , and the resulting estimated cell masses were 2.48 ng and 4.09 ng, respectively.

Table 3 shows the measured cell mass and the estimated cell mass for comparison. As shown in Table 3, the measured values and the estimated values are close to each other. One of the probable reasons for the difference was the limited growth of a

Table 3 Measured mass and estimated mass of the cells in Fig. 7

	Cell in Fig. 7(c)	Cell in Fig. 7(d)
Mass before adjustment	0.32 ng	0.62 ng
Mass after adjustment	1.01 ng	3.57 ng
Measured volume	2349 μm^3	3857 μm^3
Theoretical value	2.48 ng	4.09 ng
Ratio	41%	87%

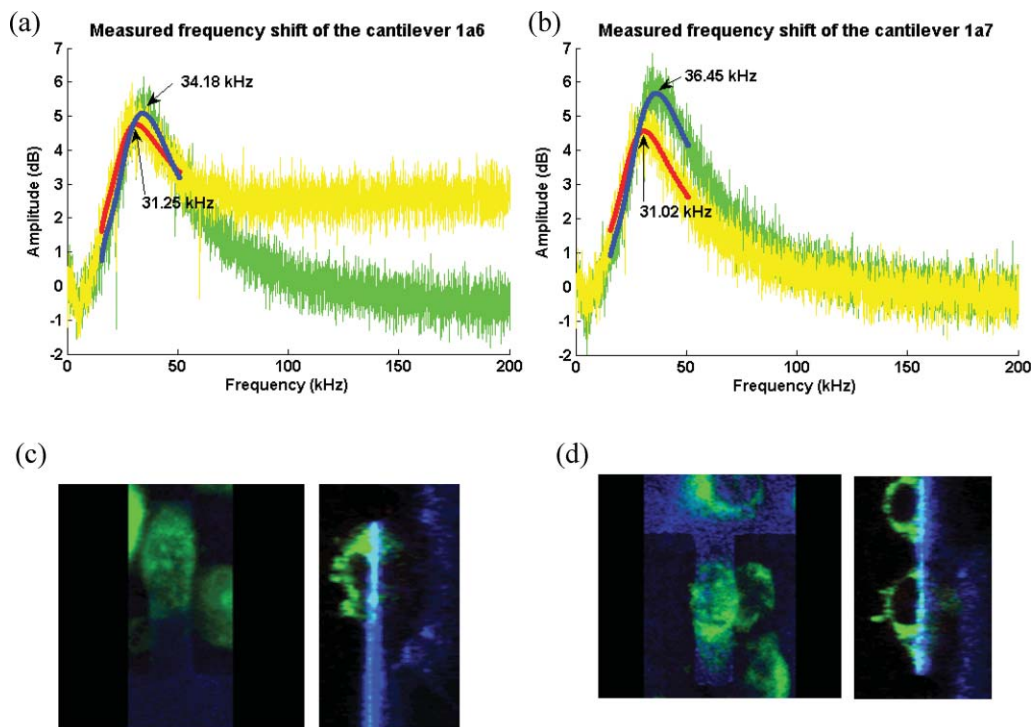


Fig. 7 Mass measurement of the attached cell. (a), (b) Measured frequency shifts due to the attached cell. (c), (d) Confocal microscope images of cultured cells on cantilevers (see ESI Fig. S1 and S2 for 3-D images of (c) and (d)†).

cell on a cantilever, due to the cantilever's small surface area, where the cell was constrained to grow only on the cantilever. The cells on the cantilevers were actually smaller than typical HeLa cells. Normally, HeLa cells occupy about 1600 μm^2 on a flat surface,³⁴ but the cells in Fig. 7 are confined on the cantilever with an area of 400 μm^2 . Also, the average volume of the HeLa cells from the literature³⁵ ranges from 4400–5000 μm^3 , whereas the cells in Fig. 7 have volumes of 2349 μm^3 and 3857 μm^3 . Therefore, the cells on the cantilevers were indeed smaller than typical HeLa cells and the density of those cells can be different from the assumed value from the literature. Also, there were a few possible error sources in the measurement and analysis process. One of the possible sources was the spring constant extracted by Sader's method.³⁰ Due to the small aspect ratio of the cantilever, the calculated spring constant can be different than the real values. However, as shown in Table 2, the values are consistent within about 10% differences to theoretical values and we can assume that this leads to at most 10% error in spring constants. Another source of the error is the resolution limit of the confocal microscopy when calculating the compensation factor for the effective mass. The average height of the cell is about 8 μm , whereas the resolution in the z -axis is 1.2 μm , which is about 15% of the cell height. Therefore, there can be roughly about $\pm 7.5\%$ error source in the correctional factor. By combining these errors, the combined error range in the measurement and analysis procedure is about $\pm 18\%$. Lastly, the assumption of uniform density of the cell body can be rather unrealistic. Due to the complex internal structures, such as the nucleus, the density can vary inside the cell body. Therefore the cell mass might not be evenly distributed and the compensated cell mass can be slightly different from the actual value.

Conclusion

In summary, we fabricated a living cantilever array to be used as a platform to characterize a single adherent cell with a non-invasive manner. The adherent cell was captured and cultured on the silicon cantilever and the mass of the cell was directly measured without detaching the cell from the surface, thus enabling the measurement of live cells in physiological conditions. Furthermore, this approach has the potential to allow the measuring of cell mass simultaneously with optical observation of single cell activities. For example, with modifications in the design of the cantilevers, the mass of cell single cells can be determined as they divide and go through a growth cycle. The living cantilever array has the potential to provide new methods to measure the cell mass in a single cell level, which could lead to a further understanding of the relationship between the size and various physiological functions of cells.

Acknowledgements

This material is based upon work supported by the National Science Foundation under Grant No. ECCS-0404107 (NSF NER) and EEC-0425626 (NSF NSEC at OSU). R. Bashir is also thankful to the BioMEMS Resources Center (NIH P41 EB002503) at the Massachusetts General Hospital for hosting a sabbatical and for partnership and collaboration. The authors would like to thank Dr Demir Akin, Weldon School of Biomedical Engineering, Purdue University, Lisa M. Reece

and Christy L. Cooper, Department of Basic Medical Sciences, Purdue University for their valuable help and advice, and Professor S. Broyles and his laboratory in the Department of Biochemistry, Purdue University for providing HeLa cells used in this study.

References

- 1 M. Godin, A. K. Bryan, T. P. Burg, K. Babcock and S. R. Manalis, *Appl. Phys. Lett.*, 2007, **91**, 123121.
- 2 T. P. Burg, M. Godin, S. M. Knudsen, W. Shen, G. Carlson, J. S. Foster, K. Babcock and S. R. Manalis, *Nature*, 2007, **446**, 1066–1069.
- 3 D. A. Wolff and H. Pertoft, *J. Cell Biol.*, 1972, **55**, 579–585.
- 4 L. H. Hartwell, *J. Bacteriol.*, 1970, **104**, 1280–1285.
- 5 J. C. Schaer and L. Ramseier, *Radiat. Res.*, 1973, **56**, 258–270.
- 6 H. Dolznig, F. Grebien, T. Sauer, H. Beug and E. W. Mullner, *Nat. Cell Biol.*, 2004, **6**, 899–905.
- 7 D. C. Fingar, S. Salama, C. Tsou, E. Harlow and J. Blenis, *Genes Dev.*, 2002, **16**, 1472–1487.
- 8 S. Floyd, C. Favre, F. M. Lasorsa, M. Leahy, G. Trigiant, P. Stroebel, A. Marx, G. Loughran, K. O'Callaghan, C. M. Marobbio, D. J. Slotboom, E. R. Kunji, F. Palmieri and R. O'Connor, *Mol. Biol. Cell*, 2007, **18**, 3545–3555.
- 9 N. Tapon, N. Ito, B. J. Dickson, J. E. Treisman and I. K. Hariharan, *Cell*, 2001, **105**, 345–355.
- 10 W. H. Coulter, US Patent 2656508, 1953.
- 11 P. F. Mullaney, M. A. Vandilla, J. R. Coulter and P. N. Dean, *Rev. Sci. Instrum.*, 1969, **40**, 1029.
- 12 S. Sergent-Tanguy, C. Chagneau, I. Neveu and P. Naveilhan, *J. Neurosci. Methods*, 2003, **129**, 73–79.
- 13 M. Segelmark, C. Barrett, W. Pendergraft, R. Falk and G. Preston, *Kidney Int.*, 2000, **57**, 1873–1881.
- 14 T. Thundat, R. J. Warmack, G. Y. Chen and D. P. Allison, *Appl. Phys. Lett.*, 1994, **64**, 2894–2896.
- 15 T. Thundat, G. Y. Chen, R. J. Warmack, D. P. Allison and E. A. Wachter, *Anal. Chem.*, 1995, **67**, 519–521.
- 16 P. S. Waggoner and H. G. Craighead, *Lab Chip*, 2007, **7**, 1238–1255.
- 17 B. Ilic, Y. Yang, K. Aubin, R. Reichenbach, S. Krylov and H. G. Craighead, *Nano Lett.*, 2005, **5**, 925–929.
- 18 A. K. Gupta, D. Akin and R. Bashir, *Appl. Phys. Lett.*, 2004, **84**, 1976–1978.
- 19 B. Ilic, Y. Yang and H. G. Craighead, *Appl. Phys. Lett.*, 2004, **85**, 2604–2606.
- 20 B. Ilic, D. Czaplowski, M. Zalalutdinov, H. G. Craighead, P. Neuzil, C. Campagnolo and C. Batt, *J. Vac. Sci. Technol., B*, 2001, **19**, 2825–2828.
- 21 A. P. Davila, J. Jang, A. K. Gupta, T. Walter, A. Aronson and R. Bashir, *Biosens. Bioelectron.*, 2007, **22**, 3028–3035.
- 22 T. Braun, V. Barwich, M. K. Ghatkesar, A. H. Bredekamp, C. Gerber, M. Hegner and H. P. Lang, *Phys. Rev. E: Stat. Phys., Plasmas, Fluids, Relat. Interdiscip. Top.*, 2005, **72**, 013907.
- 23 B. Dhayal, W. A. Henne, D. D. Doorneweerd, R. G. Reifengerger and P. S. Low, *J. Am. Chem. Soc.*, 2006, **128**, 3716–3721.
- 24 M. D. Antonik, N. P. DCosta and J. H. Hoh, *IEEE Eng. Med. Biol. Mag.*, 1997, **16**, 66–72.
- 25 K. Wilson, P. Molnar and J. Hickman, *Lab Chip*, 2007, **7**, 920–922.
- 26 J. R. Masters, *Nat. Rev.*, 2002, **2**, 315–319.
- 27 N. P. Huang, R. Michel, J. Voros, M. Textor, R. Hofer, A. Rossi, D. L. Elbert, J. A. Hubbell and N. D. Spencer, *Langmuir*, 2001, **17**, 489–498.
- 28 L. Yang, P. P. Banada, M. R. Chatni, K. Seop Lim, A. K. Bhunia, M. Ladisch and R. Bashir, *Lab Chip*, 2006, **6**, 896–905.
- 29 J. E. Sader, *J. Appl. Phys.*, 1998, **84**, 64–76.
- 30 J. E. Sader, J. W. M. Chon and P. Mulvaney, *Rev. Sci. Instrum.*, 1999, **70**, 3967–3969.
- 31 W. H. Ryu, Y. C. Chung, D. K. Choi, C. S. Yoon, C. K. Kim and Y. H. Kim, *Sens. Actuators, B*, 2004, **97**, 98–102.
- 32 S. Dohn, R. Sandberg, W. Svendsen and A. Boisen, *Appl. Phys. Lett.*, 2005, **86**, 233501.
- 33 W. G. Bardsley and J. D. Aplin, *J. Cell Sci.*, 1983, **61**, 365–373.
- 34 H. W. Fisher and T. W. Cooper, *J. Cell Biol.*, 1967, **34**, 569–576.
- 35 L. S. Cohen and Studzins. Gp, *J. Cell. Physiol.*, 1967, **69**, 331.